Available online at www.sciencedirect.com
SCIENCE DIRECT®
Journal of Solid State Chemistry 173 (2003) 1–12
JOURNAL OF SOLID STATE CHEMISTRY
http://elsevier.com/locate/jssc

# Synthesis and crystal structure of α and β-$Rb_6U_5V_2O_{23}$, a new layered compound

S. Obbade,[a,*] C. Dion,[a] L. Duvieubourg,[a] M. Saadi,[b] and F. Abraham[a]

[a] *Laboratoire de Cristallochimie et Physicochimie du Solide UMR CNRS 8012, ENSCL-USTL, BP 108, 59652 Villeneuve d'Ascq Cedex, France*
[b] *Laboratoire de Coordination et Analytique, Faculté des Sciences, Université Chouaib Doukkali, B.P. 20 El Jadida, Morocco*

Received 17 October 2002; received in revised form 12 December 2002; accepted 18 December 2002

**Abstract**

A new alkali uranyl vanadate, $Rb_6U_5V_2O_{23}$ has been synthesized by solid-state reactions. According to synthesis method, two allotropic varieties have been found and their structures determined from single-crystal X-ray diffraction data. Both compounds crystallize in the monoclinic system with space groups $C2/c$ and $P2_1/n$ for α and β varieties, respectively. α-$Rb_6U_5V_2O_{23}$ unit-cell parameters are $a = 24.887(8)$ Å, $b = 7.099(2)$ Å, $c = 14.376(4)$ Å, $\beta = 103.92(1)^\circ$, $V = 2465.2(6)$ Å$^3$, $Z = 4$, $\rho_{mes} = 5.86(2)$ g cm$^{-3}$, $\rho_{cal} = 5.85(1)$ g cm$^{-3}$ and for β-$Rb_6U_5V_2O_{23}$ $a = 7.1635(9)$ Å, $b = 14.079(2)$ Å, $c = 24.965(4)$ Å, $\beta = 90.23(1)^\circ$, $V = 2517.8(6)$ Å$^3$, $Z = 4$, $\rho_{mes} = 5.79(2)$ g cm$^{-3}$, $\rho_{cal} = 5.73(1)$ g cm$^{-3}$. A full-matrix least-squares refinement yielded, respectively, $R = 0.032$ and 0.041 for 1307 and 2276 independent reflections with $I > 2\sigma$ collected on a Smart diffractometer (Mo$K\alpha$ radiation). Both structures are characterized by $[(UO_2)_5(VO_4)_2O_5]^{6-}$ layers which are flat and parallel to the $(10\bar{1})$ plane in α variety, corrugated and parallel to the (010) plane in the β variety. The layers are built up from $VO_4$ tetrahedra and $UO_7$ pentagonal bipyramids. In β variety, $UO_6$ distorted octahedra can also be considered. The $UO_7$ pentagonal bipyramids are associated by sharing opposite equatorial edges to form zig-zag infinite chains $(UO_5)_\infty$ parallel to the *b*-axis in α variety and to the *a*-axis in β variety, respectively. These chains are linked together on one side by $VO_4$ tetrahedra and on other side in α variety by $UO_7$ pentagonal bipyramids sharing corner and opposite edges and in β variety by $UO_6$ octahedra sharing opposite edges. Both structures differ by several characteristics. In α variety, the layers are flat according to the rows of $VO_4$ tetrahedra parallel to the *b*-axis whose apical oxygen atoms are alternatively pointing on the both sides in each row whereas in β variety, they are all pointing in the same side in a row parallel to *a* and in opposite side in the next, yielding to corrugated layers.


## 1. Introduction

All the alkaline uranyl vanadate compounds studied till today have a layered structure in which uranyl and vanadate polyhedra are linked together to form planar or corrugated sheets with the alkaline ion located between the sheets. The most wide-spread structure is that of the mineral carnotite, $K(UO_2)VO_4 \cdot xH_2O$. The anhydrous carnotite and its Li, Na, Rb, Cs, Tl, Ag, $NH_4$ analogues have been synthesized [1,2]. Most of the crystal structures were refined [3–5]. This class of compounds is very large because compounds of divalent cations $M_{0.5}(UO_2)VO_4 \cdot xH_2O$ have been prepared and characterized for $M$ = Ca, Ba, Pb, Sr, Mn, Co, Ni [6–9]. The study of these materials have primarily been motivated by mineralogical interest. However, we have reported the relatively high mobility of the alkali metal ions in the $Na_{1-x}K_x(UO_2)VO_4$ $(0 \leqslant x \leqslant 1)$ solid solution [5]. This family derived from carnotite seems particularly homogeneous from a structural view point. The $UO_2^{2+}$ ions are connected by $V_2O_8^{6-}$ units formed by two inverse $VO_5$ square pyramids sharing an edge to built planar layers. They therefore have the general formula $M_{2/n}^{n+}(UO_2)_2V_2O_8 \cdot xH_2O$.

Another type of layer appears when $U/V = \frac{1}{3}$ and has been recently described for $CsUV_3O_{11}$ [10]. The layers are built from $VO_5$ square pyramids and $UO_8$ hexagonal bipyramids sharing edges and corners which extend into infinite sheets formulated $[UV_3O_{11}]_n^{n-}$ similar to the layers found in $UV_3O_{10}$ [11]. $CsUV_3O_{11}$ belongs to the class of compounds of general formula $M_{1/n}^{n+}UO_2(VO_3)_3 \cdot xH_2O$ with $M = H_3O^+$, $Na^+$, $NH_4^+$, $Mg^{2+}$ [12] which are suspected to have a layered structure on

*Corresponding author.
*E-mail address:* obbade@ensc-lille.fr (S. Obbade).

0022-4596/03/$ - see front matter © 2003 Elsevier Science (USA). All rights reserved.
doi:10.1016/S0022-4596(03)00052-5

the basis of their exchange properties. The cations, found between the $[UV_3O_{11}]^-$ layers can be exchanged for inorganic and organic cations and some water molecules can be replaced by other solvent molecules [13].

Two families of layered uranyl vanadates have been recently discovered: $M_6U_5V_2O_{23}$ with $M$ = Na, K [14] and $M_7U_8V_2O_{32}Cl$ with $M$ = Rb, Cs [15]. Single crystals of these compounds have been obtained from $(UO_2)_3(VO_4)_2 \cdot 5H_2O$ [16] towards attempts at ion "exchange" reactions in molten alkali chlorides. In $(UO_2)_3(VO_4)_2 \cdot 5H_2O$, $UO_7$ pentagonal bipyramids are associated together by the oxygen atoms of the equatorial plane of the $UO_7$ bipyramids, a $UO_7$ bipyramid shares two opposite O–O edges with two other $UO_7$ bipyramids to form zig-zag infinite chains $(UO_5)_\infty$. The parallel chains are connected by $VO_4$ tetrahedra to built slightly corrugated layers $[UO_2(VO_4)]^-$ which are linked together by disordered $UO_2^{2+}$ uranyl ions and water molecules. Reaction of this compound with molten potassium chloride led to the growth of orange single crystals of $K_6U_5V_2O_{23}$ [14]. In this compound, and the Na-analogous, the infinite $(UO_5)_\infty$ chains are preserved but the arrangement of the chains and $VO_4$ tetrahedra is different. In fact, two parallel chains are linked by oxygen atoms of the equatorial plane of the $UO_7$ pentagonal bipyramids not involved in the chain formation. In rubidium and cesium chlorides, the reaction is different and the yellow synthesized single crystals formula is $M_7U_8V_2O_{32}Cl$ [15] with $M$ = Rb, Cs. In these compounds, zig-zag chains of edge shared pentagonal bipyramids are once again obtained, but some of the oxygen atoms shared between two parallel chains are replaced by chlorine atoms. To prevent the substitution of chlorine in the double chains we have planed the use of largest anions. By reaction of $(UO_2)_3(VO_4)_2$ in an excess of molten rubidium iodide, orange single crystals of a new phase $Rb_6U_5V_2O_{23}$ are synthesized. This phase is called $\alpha$-$Rb_6U_5V_2O_{23}$ because it exhibits a transition to a $\beta$ form at high temperature. Single crystals of the $\beta$ variety of $Rb_6U_5V_2O_{23}$ have been obtained. The both crystal structures are reported in this paper and compared between them and with the other $M_6U_5V_2O_{23}$ ($M$ = Na, K) compounds.

## 2. Experimental

Single crystals of $\alpha$-$Rb_6U_5V_2O_{23}$ were prepared by reaction of uranyl orthovanadate $(UO_2)_3(VO_4)_2 \cdot 5H_2O$ prepared as described in [16] in a large excess (30/1 M accounts) of molten rubidium iodide. The mixture was slowly heated in a platinum crucible to 350°C to allow dehydration of the uranyl salt. Afterwards the temperature was increased to 650°C, above the rubidium iodide melting point, 642°C, and below that of $(UO_2)_3(VO_4)_2$, 800°C. The molten mixture was slowly cooled (5°C/h) to room temperature and washed with water to dissolve the excess of rubidium iodide, giving orange single crystals.

Attempts to synthesize powder of $\alpha$-$Rb_6U_5V_2O_{23}$ from a ternary stoichiometric mixture of $Rb_2CO_3$, $U_3O_8$ and $V_2O_5$ failed whatever the temperature. In fact, only the $\beta$ form was obtained at high temperature. The preparation of pure $\alpha$-$Rb_6U_5V_2O_{23}$ was achieved by heating a mixture of RbI (Aldrich), $U_3O_8$ (Prolabo rectapur) and $V_2O_5$ (Aldrich) in the molar ratios 6/1.67/1 at 650°C. The observed X-ray pattern of $\alpha$-$Rb_6U_5V_2O_{23}$ is in perfect agreement with the calculated pattern from the crystal structure results.

Single crystals of $\beta$-$Rb_6U_5V_2O_{23}$ have been grown from a mixture of $Rb_2CO_3$, $U_3O_8$ and $V_2O_5$ in the molar ratios 2/0.67/1 slowly heated up to 1200°C. The molten mixture was slowly cooled (10°C/h) and finally orange single crystals were obtained. From crushed crystals, a distinctive X-ray diffraction pattern was observed that characterized the allotropic variety $\beta$-$Rb_6U_5V_2O_{23}$. The powder compound was synthesized by a solid state reaction between a stoichiometric mixture of $U_3O_8$ (Prolabo rectapur), $V_2O_5$ (Aldrich) and $Rb_2CO_3$ (Aldrich) according to the following reaction:

$$\tfrac{5}{3}U_3O_8 + V_2O_5 + 3Rb_2CO_3 + \tfrac{5}{6}O_2 \rightarrow \beta - Rb_6U_5V_2O_{23} + 3CO_2.$$

The homogeneous mixture was slowly heated up to 1000°C and maintained at this temperature during 7 days with intermediate grindings and finally rapidly (150°C/h) cooled to room temperature. The X-ray diffraction pattern of the as-obtained powder is identical to that of crushed single crystals and to that of the calculated pattern from the crystal structure results.

Well shaped crystals of $\alpha$ and $\beta$-$Rb_6(UO_2)_5(VO_4)_2O_5$ were selected for structure determinations. Preliminary investigations indicated for both varieties a monoclinic symmetry. For $\alpha$ form, systematic absences of ($h\,k\,l$, $h + k = 2n + 1$ and $h\,0\,l$, $l = 2n + 1$) reflections indicated $Cc$ and $C2/c$ as possible space groups and for $\beta$, systematic absences of ($0\,k\,0$, $k + k = 2n + 1$ and $h\,0\,l$, $h + l = 2n = 1$) indicated the $P2_1/n$ space group. The structures of the two forms were solved in the centrosymmetric space groups.

Single-crystal X-ray diffraction data were collected on a BRUKER AXS diffractometer equipped with a SMART charge-coupled device (CCD) detector. Data were collected using monochromated Mo$K\alpha$ radiation. Crystal data, conditions of data collections, and structure refinement parameters are reported in Table 1 for $\alpha$ and $\beta$ forms.

The unit-cell parameters of the crushed single crystals were refined by a least-squares procedure from the indexed powder diffraction patterns, collected with a SIEMENS D5000 diffractometer (Cu$K\alpha$ radiation) equipped with a back-end monochromator and corrected for $K\alpha_2$ contribution. The figures of merit, as

Table 1
Crystal data, intensity collection and structure refinement parameters for $Rb_6(UO_2)_5(VO_4)_2O_5$

| | α-$Rb_6$ $(UO_2)_5(VO_4)_2O_5$ | | β-$Rb_6$ $(UO_2)_5(VO_4)_2O_5$ | |
|---|---|---|---|---|
| *Crystal data* | | | | |
| Crystal symmetry | Monoclinic | | Monoclinic | |
| Space group | $C2/c$ | | $P2_1/n$ | |
| Unit-cell refined from single-crystal data | $a = 24.887(8)$ Å | | 7.1635(9) Å | |
| | $b = 7.099(2)$ Å | | 14.079(2) Å | |
| | $c = 14.376(4)$ Å | | 24.965(4) Å | |
| | $\beta = 103.92(1)^\circ$ | | 90.23(1)° | |
| Unit-cell volume | 2465.2(6) $Å^3$ | | 2517.8(6) $Å^3$ | |
| $Z$ | 4 | | 4 | |
| Calculated density | $\rho = 5.85(2)$ g $cm^{-3}$ | | 5.73(1) g $cm^{-3}$ | |
| Measured density | $\rho = 5.86(2)$ g $cm^{-3}$ | | 5.79(2) g $cm^{-3}$ | |
| *Data collection* | | | | |
| Temperature (K) | 293(2) | | 293(2) | |
| Equipment | Bruker SMART CCD | | Bruker SMART CCD | |
| Radiation Mo$K\alpha$ | 0.71073 Å | | 0.71073 Å | |
| Scan mode | $\omega$ | | $\omega$ | |
| Recording $\theta$ min/max (deg) | 1.69/23.29 | | 1.63/30.03 | |
| Recording reciprocal space | $-27 \leqslant h \leqslant 27$ | | $-10 \leqslant h \leqslant 10$ | |
| | $-7 \leqslant k \leqslant 7$ | | $-18 \leqslant k \leqslant 19$ | |
| | $-15 \leqslant l \leqslant 15$ | | $-34 \leqslant l \leqslant 31$ | |
| No. of measured reflections | 5348 | | 7869 | |
| No. of independent reflections | 1307 | | 2276 | |
| $\mu$ ($cm^{-1}$) (for $\lambda K\alpha = 0.71073$ Å) | 453.14 | | 443.62 | |
| Limiting faces and distances (mm) | 1 0 0 | 0.025 | 1 0 0 | 0.064 |
| From an arbitrary origin | $\bar{1}$ 0 0 | 0.025 | $\bar{1}$ 0 0 | 0.064 |
| | 0 1 0 | 0.052 | 0 1 0 | 0.021 |
| | 0 $\bar{1}$ 0 | 0.052 | 0 $\bar{1}$ 0 | 0.021 |
| | 0 0 1 | 0.027 | 0 0 1 | 0.018 |
| | 0 0 $\bar{1}$ | 0.027 | 0 0 $\bar{1}$ | 0.018 |
| $R$ merging factor | 0.045 | | 0.067 | |
| *Refinement* | | | | |
| Refined parameters/restraints | 107/0 | | 214/0 | |
| Goodness-of-fit on $F^2$ | 1.120 | | 1.080 | |
| $R_1$ for all data | 0.0316 | | 0.0412 | |
| w$R_2$ for all data | 0.0874 | | 0.0885 | |
| Largest diffraction peak and hole(e $Å^{-3}$) | 2.16/−2.79 | | 2.00/−2.73 | |

$R_1 = \sum(|F_o| - |F_c|)/\sum|F_o|$.

$wR_2 = [\sum w(F_o^2 - F_c^2)^2/\sum w(F_o^2)^2]^{1/2}$.

$w = 1/[\sigma^2(F_o^2) + (aP)^2 + bP]$ where $a$ and $b$ are refinable parameters and $P = (F_o^2 + 2F_c^2)/3$.

defined by Smith and Snyder [17] were $F_{20} = 36(0.013; 43)$ and 28(0.010;72) for the α and β forms, respectively. The powder X-ray diffraction pattern data are reported in Tables 2 and 3, respectively.

The density, measured with an automated Micromeritics Accupyc 1330 helium pycnometer using a 1-$cm^3$ cell, indicated $Z = 4$ formula per unit cell for both α and β forms ($\rho_{exp} = 5.86(2)$ g $cm^{-3}$, $\rho_{cal} = 5.85(2)$ g $cm^{-3}$ for α; $\rho_{exp} = 5.79(2)$ g $cm^{-3}$, $\rho_{cal} = 5.73(1)$ g $cm^{-3}$ for β).

The integral intensities were extracted from the collected frames with the Bruker Saint Plus 6.02 software package [18] using a narrow-frame integration algorithm. A Gaussian-type absorption correction based on precise faces indexing was then applied using XPREP program [19] followed by SADABS [20] for additional corrections. The crystal structure of both compounds were solved by direct methods using the SHELXTL software [19], which gave the position of U, Rb and V atoms. Oxygen positions were deduced from subsequent refinements and difference Fourier maps calculation. Both structures were refined on the basis of $F^2$ for all unique data, using the SHELXL program. Refinement of atomic positional parameters, anisotropic displacement parameters for U, V, Rb atoms, and isotropic displacement for O atoms yielded to final $R_1 = 0.0316$ and $wR_2 = 0.0874$ for 1307 independent reflections for α-$Rb_6U_5V_2O_{23}$ and $R_1 = 0.0412$, $wR_2 = 0.0885$ for 2276 independent reflections for β-$Rb_6U_5V_2O_{23}$. The atomic positions and equivalent isotropic displacement factors and anisotropic displacement parameters for metals are reported in Tables 4 and 5 for the α and in Tables 6 and 7 for the β form, respectively.

Table 2
Observed and calculated X-ray powder diagram α-$Rb_6U_5V_2O_{23}$

| $h\,k\,l$ | $2\theta$ obs. | $2\theta$ cal. | Intensity % | $h\,k\,l$ | $2\theta$ obs. | $2\theta$ cal. | Intensity % |
|---|---|---|---|---|---|---|---|
| 2 0 −2 | 13.079 | 13.045 | 80 | 7 1 0 | 28.814 | 28.804 | 90 |
| 1 1 −1 | 14.053 | 14.079 | 5 | 2 2 2 | 29.975 | 29.968 | 8 |
| 4 0 0 | 14.730 | 14.695 | 16 | 2 2 −3 | 31.491 | 31.481 | 13 |
| 2 0 2 | 16.178 | 16.154 | 12 | 5 1 3 | 32.355 | 32.366 | 4 |
| 1 1 2 | 18.833 | 18.824 | 5 | 3 1 4 | 32.874 | 32.895 | 23 |
| 4 0 2 | 21.760 | 21.745 | 6 | 4 2 −3 | 33.019 | 33.014 | 7 |
| 5 1 0 | 22.295 | 22.281 | 17 | 9 1 2 | 35.215 | 35.199 | 21 |
| 3 1 2 | 22.611 | 22.583 | 11 | 6 0 −6 | 39.832 | 39.849 | 12 |
| 6 0 −2 | 22.734 | 22.713 | 6 | 9 1 2 | 40.932 | 40.921 | 12 |
| 2 0 −4 | 24.840 | 24.821 | 15 | 1 1 6 | 41.915 | 41.932 | 14 |
| 0 2 0 | 25.107 | 25.070 | 15 | 5 3 0 | 42.512 | 42.530 | 19 |
| 0 0 4 | 25.550 | 25.561 | 24 | 8 0 −6 | 43.042 | 43.029 | 19 |
| 0 2 1 | 25.896 | 25.885 | 35 | 5 3 1 | 43.747 | 43.759 | 32 |
| 4 0 −4 | 26.271 | 26.263 | 75 | 11 1 −4 | 45.067 | 45.055 | 16 |
| 2 2 −1 | 26.516 | 26.502 | 20 | 10 2 −3 | 45.726 | 45.766 | 7 |
| 3 1 3 | 27.425 | 27.426 | 37 | 3 1 −7 | 46.054 | 46.035 | 18 |
| 5 1 2 | 27.902 | 27.899 | 100 | 7 3 0 | 46.539 | 46.539 | 8 |
| 7 1 −1 | 28.110 | 28.101 | 40 | 6 2 −6 | 47.631 | 47.660 | 15 |
| 2 2 −2 | 28.384 | 28.360 | 78 | 7 3 1 | 47.911 | 47.950 | 11 |

Table 3
Observed and calculated X-ray powder diagram β-$Rb_6U_5V_2O_{23}$

| $h\,k\,l$ | $2\theta$ obs. | $2\theta$ calc. | Intensity % | $h\,k\,l$ | $2\theta$ obs. | $2\theta$ cal. | Intensity % |
|---|---|---|---|---|---|---|---|
| 0 0 2 | 7.082 | 7.079 | 17 | 2 1 4 | 29.482 | 29.487 | 19 |
| 0 1 3 | 12.371 | 12.351 | 21 | 1 2 7 | 30.801 | 30.786 | 29 |
| 0 2 0 | 12.583 | 12.570 | 37 | 0 2 8 | 31.342 | 31.343 | 5 |
| 1 0 1 | 12.853 | 12.866 | 18 | 0 3 7 | 31.483 | 31.494 | 7 |
| 0 2 1 | 13.081 | 13.062 | 23 | 2 2 4 | 31.524 | 31.516 | 5 |
| 1 1 0 | 13.852 | 13.863 | 10 | 2 3 1 | 31.633 | 31.626 | 8 |
| 0 2 2 | 14.452 | 14.440 | 22 | 1 4 4 | 31.754 | 31.744 | 8 |
| 1 1 −2 | 15.570 | 15.556 | 8 | 2 3 3 | 33.262 | 33.280 | 5 |
| 0 2 3 | 16.500 | 16.488 | 6 | 1 4 5 | 33.600 | 33.588 | 28 |
| 0 2 5 | 21.822 | 21.815 | 15 | 1 3 −8 | 36.711 | 36.730 | 5 |
| 1 1 5 | 22.650 | 22.643 | 7 | 3 0 −5 | 41.846 | 41.837 | 6 |
| 0 2 6 | 24.852 | 24.848 | 5 | 3 1 −5 | 42.362 | 42.349 | 26 |
| 1 2 5 | 25.140 | 25.160 | 57 | 0 2 12 | 45.451 | 45.444 | 15 |
| 2 1 0 | 25.632 | 25.649 | 35 | 1 3 −11 | 46.112 | 46.130 | 13 |
| 0 1 7 | 25.742 | 25.759 | 44 | 2 4 −8 | 46.310 | 46.323 | 23 |
| 2 1 1 | 25.912 | 25.917 | 27 | 0 7 3 | 46.431 | 46.430 | 6 |
| 0 4 2 | 26.315 | 26.298 | 23 | 3 4 6 | 51.224 | 51.232 | 4 |
| 2 1 2 | 26.660 | 26.672 | 13 | 3 5 −3 | 51.292 | 51.291 | 3 |
| 1 3 4 | 26.865 | 26.849 | 26 | 2 6 −6 | 51.414 | 51.401 | 18 |
| 0 4 3 | 27.511 | 27.504 | 37 | 0 8 0 | 51.922 | 51.937 | 8 |
| 1 0 7 | 27.992 | 27.982 | 100 | 0 2 14 | 52.944 | 52.950 | 7 |
| 1 4 0 | 28.214 | 28.226 | 17 | 4 0 −4 | 53.111 | 53.109 | 4 |
| 0 3 6 | 28.632 | 28.641 | 63 | 3 3 −9 | 54.182 | 54.187 | 20 |
| 1 3 5 | 28.947 | 28.957 | 39 | 3 6 0 | 54.810 | 54.808 | 21 |

$a = 7.162(1)$ Å, $b = 14.073(2)$ Å, $c = 24.954(3)$ Å, $\beta = 90.27(1)$ Å, $F_{20} = 28(0.010; 72)$.

## 3. Description of the structures and discussion

### 3.1. α-$Rb_6U_5V_2O_{23}$

Table 8 provides for α-$Rb_6U_5V_2O_{23}$ the most significant distances, angles and bond valence sums calculated using Brese and O'Keeffe's data [21] with $b = 0.37$ Å except for U–O bonds where the coordination independent parameters ($R_{ij} = 2.051$ Å and $b = 0.519$ Å) were taken from Burns et al. [22].

The three independent uranium atoms U(1), U(2) and U(3) are bonded to two oxygen atoms at short distances, O(4) and O(5) for U(1), O(2) and O(3) for U(2), and two O(1) for U(3), respectively, forming nearly linear uranyl

ions, $U(1)O_2^{2+}$, $U(2)O_2^{2+}$, and $U(3)O_2^{2+}$, Fig. 1. The three uranyl ions are surrounded in the equatorial plane by a pentagonal environment of oxygen atoms thus all coordination polyhedra of U atoms are pentagonal bipyramids $UO_7$. The uranyl-ion bond lengths range from 1.797(13) to 1.854(14) Å with an average value of 1.834 Å. The remaining equatorial oxygen ligands show significant variations with U–O distances ranging from 2.219(12) to 2.406(13) Å for $U(1)O_7$, from 2.156(7) to 2.762(12) Å for $U(2)O_7$ and from 2.230(12) to 2.800(21) Å for $U(3)O_7$, respectively. However, the average values, 2.337, 2.340, 2.375 Å for U(1), U(2), U(3) polyhedra, respectively, are in good agreement with the average bond length of 2.37(9) Å calculated for uranyl polyhedra of numerous well-refined structures [22]. The $UO_7$ polyhedra share edges to form $[(UO_2)_5O_{11}]_\infty$ infinite ribbons three uranium polyhedra width parallel to the $(10\bar{1})$ plane and running along *b*-axis. Vanadium is tetrahedrally coordinated with V–O distances ranging from 1.631(15) to 1.804(13) Å. Two $[(UO_2)_5O_{11}]_\infty$ ribbons are linked together by $VO_4$ tetrahedra. Each $VO_4$ tetrahedron shares an O(6)–O(10) edge with an $U(2)O_7$ pentagonal bipyramid of one ribbon and an O(8) corner with an $U(1)O_7$ bipyramid of the neighboring ribbon. The $VO_4$ tetrahedron is highly distorted, the shortest V–O distance involving the non-shared oxygen atom. Uranyl pentagonal bipyramids and vanadium tetrahedra form planar layers parallel to the $(10\bar{1})$ plane. Fig. 1 shows a representation of a layer in this plane. The layers are stacked along the *c*-axis. Fig. 2 represents an orthogonal projection of the structure in the (010) plane. Rubidium ions lie in the interlayer space and ensure the cohesion between the layers. Except the Rb(3)–O(8) bond, all the oxygen atoms participating to the rubidium coordination polyhedra are uranyl oxygen or the non-shared O(11) atom of the $VO_4$ tetrahedron.

Table 4
Atomic positions, isotropic thermal factors of α-$Rb_6$ $(UO_2)_5(VO_4)_2O_5$

| Atom | Site. | *x* | *y* | *z* | $U_{iso}$, $U_{eq}$* |
|---|---|---|---|---|---|
| U1 | 8*f* | 0.14618(2) | 0.03641(9) | 0.88365(4) | 0.0069(2)* |
| U2 | 8*f* | 0.08314(2) | −0.44550(9) | 0.82897(4) | 0.0068(2)* |
| U3 | 4*e* | 0 | 0.09559(9) | 3/4 | 0.0081(3)* |
| V | 8*f* | 0.28199(9) | −0.0479(4) | 1.0694(2) | 0.0075(6)* |
| Rb1 | 8*f* | 0.03557(7) | 0.2467(2) | 1.05248(9) | 0.0184(4)* |
| Rb2 | 8*f* | 0.13083(8) | 0.2532(2) | 0.61466(9) | 0.0185(5)* |
| Rb3 | 8*f* | 0.29099(8) | 0.2199(3) | 0.82973(9) | 0.0207(5)* |
| O1 | 8*f* | 0.0232(5) | 0.1024(9) | 0.6375(8) | 0.013(3) |
| O2 | 8*f* | 0.0626(5) | −0.4554(9) | 0.9446(9) | 0.016(3) |
| O3 | 8*f* | 0.1083(5) | −0.4288(9) | 0.7182(9) | 0.016(3) |
| O4 | 8*f* | 0.1297(5) | 0.0690(9) | 0.9989(9) | 0.018(3) |
| O5 | 8*f* | 0.1651(5) | 0.0087(9) | 0.7714(8) | 0.015(3) |
| O6 | 8*f* | 0.3375(5) | −0.2159(9) | 1.0800(8) | 0.015(3) |
| O7 | 8*f* | −0.0646(5) | −0.1286(9) | 0.6815(8) | 0.014(3) |
| O8 | 8*f* | 0.2432(5) | −0.0042(9) | 0.9561(9) | 0.017(3) |
| O9 | 8*f* | 0.0792(5) | 0.2380(9) | 0.8205(8) | 0.018(3) |
| O10 | 8*f* | 0.3202(5) | 0.1493(9) | 1.1107(9) | 0.018(3) |
| O11 | 8*f* | 0.2417(5) | −0.1004(9) | 1.1399(9) | 0.019(3) |
| O12 | 4*e* | 0 | −0.5100(9) | 3/4 | 0.023(4) |

*Note*. The $U_{eq}$ values are defined by $U_{eq} = \frac{1}{3}\left(\sum_i \sum_j U_{ij} a_i^* a_j^* a_i a_j\right)$.

### 3.2. β-$Rb_6U_5V_2O_{23}$

Table 9 provides for β-$Rb_6U_5V_2O_{23}$ the most significant distances, angles and bond valence sums.

Each of the five independent uranium atoms is bonded to two oxygen atoms at short distance, O(1) and O(5) for U(1), O(8) and O(2) for U(2), O(11) and O(3) for U(3), O(4) and O(9) for U(4), O(20) and O(10) for U(5), respectively, forming nearly linear uranyl ions $UO_2^{2+}$. The uranyl-ion bond lengths range from 1.746(13) to 1.867(14) Å with an average value of 1.820 Å. As excepted for U(3), uranyl ions are surrounded in the equatorial plane by a pentagonal environment of oxygen atoms; thus the coordination polyhedra of these uranium atoms are pentagonal bipyramids. The equatorial oxygen ligands show significant variations with U–O distances ranging from 2.106(22) to 2.642(24) Å, however the average values, 2.355, 2.338, 2.309 and 2.338 Å for U(1), U(2), U(4) and U(5) polyhedra, respectively, are in good agreement with the average bond length of 2.37(9) Å [22]. For the U(3) atom, the coordination polyhedron is a distorted octahedron with two oxygen atoms at shorter distance belonging to the uranyl $U(3)O_2^{2+}$ ion and four oxygen atoms at longer distances (ranging from 2.251(23) to

Table 5
Thermal anisotropic factors for metals (U, V, Rb) of α-$Rb_6$ $(UO_2)_5(VO_4)_2O_5$ (Å$^2$)

| Atom | $U_{11}$ | $U_{22}$ | $U_{33}$ | $U_{12}$ | $U_{13}$ | $U_{23}$ |
|---|---|---|---|---|---|---|
| U1 | 0.0082(4) | 0.0111(4) | 0.0026(4) | 0.0009(3) | 0.0035(3) | 0.0005(3) |
| U2 | 0.0074(4) | 0.0112(4) | 0.0030(4) | −0.0009(3) | 0.0039(3) | −0.0005(2) |
| U3 | 0.0075(5) | 0.0153(5) | 0.0028(5) | 0.00000 | 0.0039(4) | 0.00000 |
| V | 0.0050(14) | 0.0113(15) | 0.0074(16) | 0.0020(12) | 0.0037(12) | 0.0002(12) |
| Rb1 | 0.021(1) | 0.0205(10) | 0.0161(10) | 0.0000(8) | 0.0093(8) | 0.0017(7) |
| Rb2 | 0.027(1) | 0.0199(10) | 0.0100(9) | 0.0037(8) | 0.0071(8) | 0.0003(7) |
| Rb3 | 0.026(1) | 0.0227(10) | 0.0184(10) | 0.0013(8) | 0.0155(8) | −0.0001(8) |

*Note*. The anisotropic displacement factor exponent takes the form $-2\pi^2[h^2a*^2 U_{11} + \cdots + 2hka*b* U_{12}]$.

2.310(21) Å) in the equatorial plane, forming a trapezoid, the distance to the fifth equatorial oxygen atom O(23) (3.31 Å) is too long to be considered as a bond.

Table 6
Atomic positions, isotropic thermal factors (Å$^2$) of $\beta$-$Rb_6$ $(UO_2)_5$ $(VO_4)_2O_5$

| Atom | Site | $x$ | $y$ | $z$ | $U_{iso}$, $U_{eq}$* |
|---|---|---|---|---|---|
| U1 | 4*e* | 0.82487(9) | 0.22872(9) | 0.04327(5) | 0.0097(3)* |
| U2 | 4*e* | 0.82249(9) | 0.31502(9) | −0.11968(5) | 0.0110(3)* |
| U3 | 4*e* | 0.33905(9) | 0.27449(9) | −0.03742(5) | 0.0116(3)* |
| U4 | 4*e* | 1.31574(9) | 0.19707(9) | 0.10343(5) | 0.0104(3)* |
| U5 | 4*e* | 1.31324(9) | 0.33203(9) | −0.18011(5) | 0.0117(3)* |
| V1 | 4*e* | 0.8228(7) | 0.1408(4) | 0.1671(2) | 0.015(1)* |
| V2 | 4*e* | 0.8129(7) | 0.3883(4) | −0.2441(2) | 0.007(1)* |
| Rb1 | 4*e* | 0.4937(4) | 0.5335(2) | −0.0808(1) | 0.0196(8)* |
| Rb2 | 4*e* | 0.0069(5) | 0.0586(3) | −0.0770(1) | 0.0235(8)* |
| Rb3 | 2*d* | 1.5 | 0 | 0 | 0.0203(9)* |
| Rb4 | 2*c* | 0 | 1/2 | 0 | 0.0248(9)* |
| Rb5 | 4*e* | 1.4829(5) | −0.0562(3) | 0.1533(1) | 0.0240(8)* |
| Rb6 | 4*e* | 0.9847(5) | 0.3972(3) | 0.1702(1) | 0.0378(9)* |
| Rb7 | 4*e* | 0.9971(5) | 0.1327(3) | −0.2497(2) | 0.0345(9)* |
| O1 | 4*e* | 0.825(3) | 0.1020(9) | 0.0233(8) | 0.008(5) |
| O2 | 4*e* | 0.831(3) | 0.4433(9) | −0.1050(9) | 0.019(6) |
| O3 | 4*e* | 0.338(3) | 0.3972(9) | −0.0145(8) | 0.008(5) |
| O4 | 4*e* | 1.295(3) | 0.0738(9) | 0.0849(9) | 0.019(6) |
| O5 | 4*e* | 0.824(3) | 0.3528(9) | 0.0696(9) | 0.021(6) |
| O6 | 4*e* | 1.140(3) | 0.3115(9) | −0.1042(8) | 0.014(5) |
| O7 | 4*e* | 0.514(3) | 0.3242(9) | −0.1097(7) | 0.007(4) |
| O8 | 4*e* | 0.816(3) | 0.1906(9) | −0.1400(8) | 0.015(5) |
| O9 | 4*e* | 1.324(3) | 0.3202(9) | 0.1282(9) | 0.020(5) |
| O10 | 4*e* | 1.311(3) | 0.4598(9) | −0.1763(9) | 0.020(5) |
| O11 | 4*e* | 0.350(3) | 0.1522(9) | −0.0589(9) | 0.027(6) |
| O12 | 4*e* | 0.633(3) | 0.1634(9) | 0.1256(9) | 0.019(5) |
| O13 | 4*e* | 0.812(3) | 0.5055(9) | −0.2481(9) | 0.025(6) |
| O14 | 4*e* | 0.853(3) | 0.0215(9) | 0.1728(9) | 0.021(6) |
| O15 | 4*e* | 0.631(3) | 0.3450(9) | −0.2067(9) | 0.024(6) |
| O16 | 4*e* | 1.140(3) | 0.2375(9) | 0.0290(8) | 0.016(5) |
| O17 | 4*e* | 0.510(3) | 0.2298(9) | 0.0358(9) | 0.020(5) |
| O18 | 4*e* | 0.996(3) | 0.3448(9) | −0.2001(8) | 0.013(5) |
| O19 | 4*e* | 1.006(4) | 0.1936(9) | 0.1254(8) | 0.036(7) |
| O20 | 4*e* | 1.304(3) | 0.2088(9) | −0.1877(9) | 0.024(6) |
| O21 | 4*e* | 0.818(3) | 0.3433(9) | −0.3065(9) | 0.023(6) |
| O22 | 4*e* | 0.803(3) | 0.1920(9) | 0.2239(9) | 0.029(6) |
| O23 | 4*e* | 0.801(3) | 0.2760(9) | −0.0365(9) | 0.033(6) |

The $UO_7$ and $UO_6$ polyhedra share edges to form $[(UO_2)_5O_{11}]_\infty$ infinite ribbons three uranium polyhedra width. Both independent vanadium atoms V(1) and V(2) are tetrahedrally coordinated with V–O distances ranging from 1.598(22) to 1.836(26) Å for V(1) and from 1.653(14) to 1.814(22) Å for V(2). Two consecutive $[(UO_2)_5O_{11}]_\infty$ ribbons are connected by $VO_4$ tetrahedra. Each tetrahedron shares an edge with one $UO_7$ pentagonal bipyramid of one ribbon and a vertex with an $UO_7$ polyhedron of the consecutive ribbon. Corrugated layers parallel to the (010) plane are formed, Fig. 3. The seven independent rubidium ions occupy the interlayer space and ensure the cohesion of the structure, Fig. 4. All the Rb–O distances lower than 3.0 Å involve uranyl oxygen or the non-shared O(13) and O(14) atoms of the $VO_4$ tetrahedra.

### 3.3. Comparison between α and β-$Rb_6U_5V_2O_{23}$ and other uranyl vanadates

To compare the structures of the two forms of $Rb_6U_5V_2O_{23}$ with those of other uranyl-containing compounds it is interesting to consider the infinite zig-zag chains $(UO_5)_\infty$ formed by sharing opposite equatorial edges of $UO_7$ pentagonal bipyramids. These chains, running along the *b*-axis, result from edge-sharing between $U(1)O_7$ and $U(2)O_7$ entities in α-$Rb_6U_5V_2O_{23}$. In the β form two kinds of chains are formed from edge-sharing between $U(1)O_7$ and $U(4)O_7$ entities and between $U(2)O_7$ and $U(5)O_7$, respectively. These chains are similar to those found in well-known compounds such α-$U_3O_8$ [23], $UVO_5$ [4,24,25], $USbO_5$ [26], $UMo_2O_8$ [27], umohoite $UMoO_6 \cdot 2H_2O$ [28], uranyl silicate minerals such as weeksite [29] and other recently studied compounds like $U_2P_2O_{10}$ [30], uranyl divanadate $(UO_2)_2V_2O_7$ [31,32], hydrated uranyl orthovanadate $(UO_2)_3(VO_4)_2 \cdot 5H_2O$ [16] and orthophosphate $(UO_2)_3(PO_4)_2 \cdot 4H_2O$ [33], $M_6U_5V_2O_{23}$ ($M$ = K, Na) [14]. While in the majority of the cases, chains are connected

Table 7
Thermal anisotropic factors for metals (U, V, Rb) of β-$Rb_6$ $(UO_2)_5(VO_4)_2O_5$ (Å$^2$)

| Atom | $U_{11}$ | $U_{22}$ | $U_{33}$ | $U_{12}$ | $U_{13}$ | $U_{23}$ |
|---|---|---|---|---|---|---|
| U1 | 0.0068(6) | 0.0134(7) | 0.0090(6) | 0.0005(5) | −0.0011(5) | −0.0001(6) |
| U2 | 0.0063(6) | 0.0136(7) | 0.0131(6) | −0.0001(5) | 0.0000(5) | 0.0020(6) |
| U3 | 0.0131(6) | 0.0134(7) | 0.0082(6) | −0.0008(5) | −0.0009(5) | 0.0016(5) |
| U4 | 0.0074(6) | 0.0116(7) | 0.0121(6) | −0.0001(5) | 0.0010(5) | 0.0016(5) |
| U5 | 0.0116(6) | 0.0138(7) | 0.0097(6) | −0.0001(5) | −0.0009(5) | 0.0022(5) |
| V1 | 0.002(3) | 0.029(4) | 0.016(3) | −0.001(2) | 0.000(2) | 0.015(3) |
| V2 | 0.003(3) | 0.008(3) | 0.009(3) | −0.001(2) | 0.000(2) | 0.001(2) |
| Rb1 | 0.018(2) | 0.019(2) | 0.022(2) | −0.001(1) | 0.002(1) | 0.001(1) |
| Rb2 | 0.019(2) | 0.024(2) | 0.028(2) | 0.001(1) | −0.002(1) | 0.001(1) |
| Rb3 | 0.020(3) | 0.023(3) | 0.018(2) | −0.002(2) | −0.001(2) | −0.002(2) |
| Rb4 | 0.018(3) | 0.033(3) | 0.024(3) | 0.003(2) | 0.003(2) | 0.005(2) |
| Rb5 | 0.026(2) | 0.022(2) | 0.024(2) | 0.004(1) | −0.0022(15) | 0.001(1) |
| Rb6 | 0.025(2) | 0.050(3) | 0.039(2) | 0.009(2) | −0.008(2) | −0.025(2) |
| Rb7 | 0.027(2) | 0.040(3) | 0.037(2) | −0.009(2) | −0.002(1) | −0.009(2) |

Table 8
Bond distances (Å), angles (deg) and bond valences $S_{ij}$ in α-$Rb_6(UO_2)_5(VO_4)_2O_5$

| *U environment* | | | | |
|---|---|---|---|---|
| | | $S_{ij}$ | | |
| U1–O5 | 1.797(13) | 1.632 | | |
| U1–O4 | 1.815(14) | 1.576 | O5–U1–O4 | 177.7(5) |
| U1–O9 | 2.219(12) | 0.723 | O5–U1–O9 | 92.1(4) |
| U1–O7$^{i}$ | 2.336(12) | 0.577 | O5–U1–O7$^{i}$ | 88.6(4) |
| U1–O6$^{ii}$ | 2.348(12) | 0.564 | O5–U1–O6$^{ii}$ | 91.4(3) |
| U1–O10$^{iii}$ | 2.377(12) | 0.534 | O5–U1–O10$^{iii}$ | 88.1(4) |
| U1–O8 | 2.406(13) | 0.505 | O5–U1–O8 | 85.6(5) |
| $\sum S_{ij}$ | | 6.110 | | |
| U2–O3 | 1.850(14) | 1.473 | | |
| U2–O2 | 1.854(14) | 1.459 | O3–U2–O2 | 176.0(5) |
| U2–O12 | 2.156(7) | 0.815 | O3–U2–O12 | 92.3(4) |
| U2–O9$^{vi}$ | 2.251(12) | 0.680 | O3–U2–O9$^{vi}$ | 92.1(3) |
| U2–O7$^{i}$ | 2.294(12) | 0.626 | O3–U2–O7$^{i}$ | 89.2(3) |
| U2–O6$^{ii}$ | 2.384(12) | 0.526 | O3–U2–O6$^{ii}$ | 91.9(4) |
| U2–O10$^{ii}$ | 2.762(12) | 0.254 | O3–U2–O10$^{ii}$ | 81.6(4) |
| $\sum S_{ij}$ | | 5.833 | | |
| U3–O1 | 1.844(13) | 1.493 | | |
| U3–O1$^{i}$ | 1.844(13) | 1.493 | O1–U3–O1$^{i}$ | 177.0(5) |
| U3–O9$^{i}$ | 2.230(12) | 0.708 | O1–U3–O9$^{i}$ | 91.1(4) |
| U3–O9 | 2.230(12) | 0.708 | O1–U3–O9 | 87.6(4) |
| U3–O7 | 2.308(12) | 0.609 | O1–U3–O7 | 88.7(4) |
| U3–O7$^{i}$ | 2.308(12) | 0.609 | O1–U3–O7$^{i}$ | 93.4(4) |
| U3–O12$^{v}$ | 2.800(21) | 0.237 | O1–U3–O12$^{v}$ | 88.5(2) |
| $\sum S_{ij}$ | | 5.857 | | |
| *V tetrahedral environment* | | | | |
| V–O11 | 1.631(15) | 1.592 | O11–V–O8 | 110.0(6) |
| V–O8 | 1.710(13) | 1.286 | O11–V–O10 | 110.1(5) |
| V–O10 | 1.716(12) | 1.265 | O11–V–O6 | 111.7(5) |
| V–O6 | 1.804(13) | 1.000 | O8–V–O10 | 108.7(5) |
| $\sum S_{ij}$ | | 5.14 | O8–V–O6 | 116.5(5) |

| *Rb environment* | | $S_{ij}$ | | | $S_{ij}$ | | | $S_{ij}$ |
|---|---|---|---|---|---|---|---|---|
| Rb1–O2$^{v}$ | 2.799(11) | 0.236 | Rb2–O5 | 2.809(12) | 0.229 | Rb3–O11$^{xi}$ | 2.839(16) | 0.211 |
| Rb1–O1$^{iv}$ | 2.813(8) | 0.226 | Rb2–O4$^{xi}$ | 2.825(9) | 0.220 | Rb3–O5$^{xii}$ | 2.877(12) | 0.191 |
| Rb1–O2$^{vii}$ | 2.866(12) | 0.196 | Rb2–O3$^{v}$ | 2.833(10) | 0.214 | Rb3–O8 | 2.878(14) | 0.190 |
| Rb1–O4 | 2.922(14) | 0.168 | Rb2–O11$^{xi}$ | 2.905(12) | 0.176 | Rb3–O11$^{iii}$ | 2.884(8) | 0.187 |
| Rb1–O3$^{iv}$ | 2.924(18) | 0.168 | Rb2–O11$^{xi}$ | 2.905(12) | 0.146 | Rb3–O3$^{xii}$ | 2.950(14) | 0.156 |
| Rb1–O1$^{i}$ | 2.954(17) | 0.154 | Rb2–O1 | 2.975(13) | 0.141 | Rb3–O4$^{iii}$ | 3.142(18) | 0.093 |
| Rb1–O7$^{iv}$ | 3.547(18) | 0.031 | Rb2–O2$^{xi}$ | 2.987(17) | 0.106 | Rb3–O10$^{iii}$ | 3.224(15) | 0.075 |
| $\sum S_{ij}$ | | 1.179 | | | 1.267 | | | 1.103 |

Symmetry codes: (i) $-x, y, 1.5-z$; (ii) $0.5-x, -0.5-y, 2-z$; (iii) $0.5-x, 0.5-y, 2-z$; (iv) $x, -y, 0.5+z$; (v) $x, 1+y, z$; (vi) $x, -1+y, z$; (vii) $-x, -y, 2-z$; (viii) $-x, 1+y, 1.5-z$; (ix) $0.5-x, -0.5+y, 1.5-z$; (x) $-x, 1-y, 2-z$; (xi) $x, -y, -0.5+z$; (xii) $0.5-x, 0.5+y, 1.5-z$.

by polyhedra such as $VO_4$ tetrahedra in $(UO_2)_3(VO_4)_2 \cdot 5H_2O$ [16], $VO_5$ square pyramids in $UVO_5$ [4,24,25], $SbO_6$ octahedra in $USbO_5$ [26] or distorted $MoO_5(OH)$ in umohoite [28], $ReO_3$-type slabs of two-octahedra wide in $UMo_2O_8$ [27], divanadate groups in $U_2V_2O_{11}$ [31,32], silicate tetrahedra chains in weeksite [29], in α and β forms of $Rb_6U_5V_2O_{23}$ they are connected by corner sharing to form double chains similar to those found in the series $M_6U_5V_2O_{23}$ ($M$ = K, Na) [14]. Within the double chains very distorted hexagonal rings better described as a quadrangular site flanked by two triangular sites are created. The quadrangular site is occupied by a U atom when the triangular sites are empties. The coordination of the "inserted" U atom is related to the distortion of the oxygen six-membered cycle. The distortion can be measured by the angle between the two O–O edges labeled O1–O2 in Figs. 5 and 6 and Table 10. In $K_6U_5V_2O_{23}$ the quadrangular site is perfectly rectangular, the U atom occupies the center of the rectangle with four relatively short U–O distances (2.28(2)2× and 2.29(2)2× Å), the two other U–O distances are very long (3.568(17) Å), so the

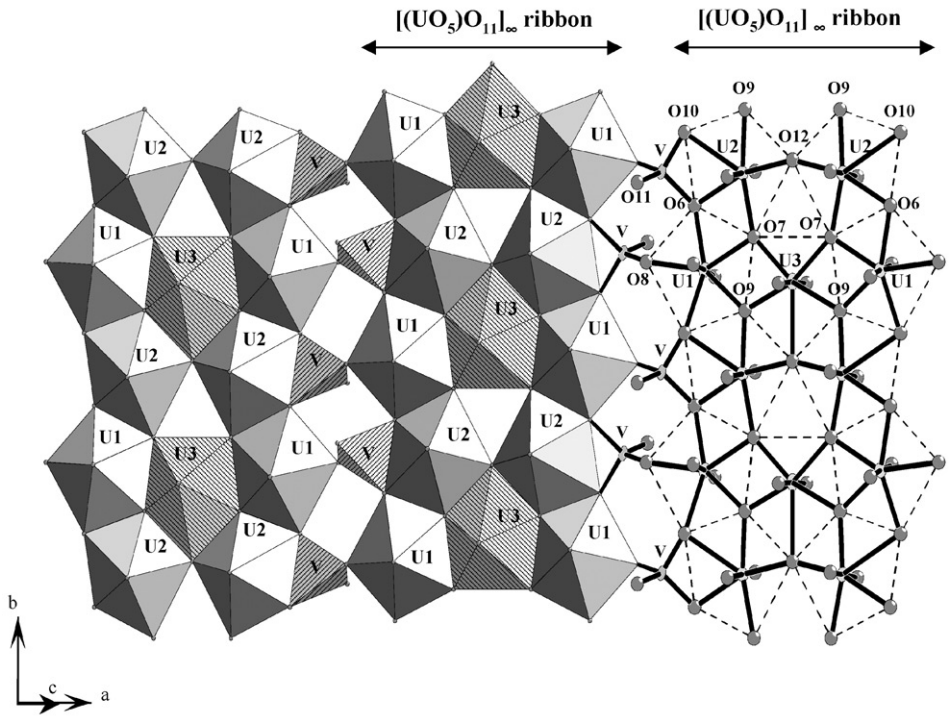


Fig. 1. Projection of the $(U_5V_2O_{23})^{6-}$ layer of α-$Rb_6U_5V_2O_{23}$ on $(10\bar{1})$ plane showing the three polyhedra width ribbons built from edge-shared $UO_7$ pentagonal bipyramids connected by $VO_4$ tetrahedra.

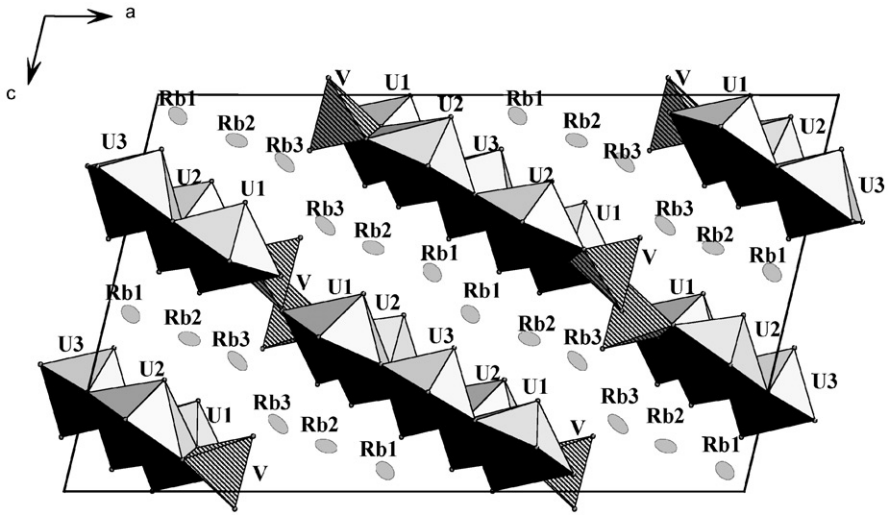


Fig. 2. Projection of the crystal structure of α-$Rb_6U_5V_2O_{23}$ on (010) plane showing the planar $(U_5V_2O_{23})^{6-}$ layers and interlayer Rb atoms.

coordination of the U atom is unambiguously octahedral. For the other $M_6U_5V_2O_{23}$ ($M$ = Na, Rb) compounds the deformation of the $(UO_5)_\infty$ chains creates a trapezium site rather than rectangular (Fig. 5) and leads to the coming together of an oxygen atom of the triangular site (Table 10) leading to a modification of the uranium environment from a distorted octahedron to a pentagonal bipyramid. This fact is illustrated well in the structures of the α and β forms of $Rb_6U_5V_2O_{23}$, the deformation of chains is more important in the α form, the environment of the uranium U(3) is a pentagonal bipyramid while in the β phase it is rather an octahedron. The more important deformation of the chains is observed in $\alpha U_3O_8$ [25] with an angle between the O–O edges of 24.98°, the distance of the fifth oxygen atom in the equatorial plane of the uranium coordination being 2.442(21) Å. In this compound the linkage between $(UO_5)_\infty$ chains is not limited to two chains and

Table 9
Bond distances (Å), angles (deg) and bond valences $S_{ij}$ in $\beta$-$Rb_6(UO_2)_5(VO_4)_2O_5$

| | | | | |
|---|---|---|---|---|
| *U environment* | | | | |
| | | $S_{ij}$ | | |
| U1–O1 | 1.852(13) | 1.473 | | |
| U1–O5 | 1.867(14) | 1.417 | O1–U1–O5 | 175.0(6) |
| U1–O23 | 2.106(22) | 0.910 | O1–U1–O23 | 92.9(7) |
| U1–O17 | 2.263(22) | 0.669 | O1–U1–O17 | 89.2(7) |
| U1–O16 | 2.290(22) | 0.631 | O1–U1–O16 | 90.5(7) |
| U1–O19 | 2.472(25) | 0.446 | O1–U1–O19 | 91.7(7) |
| U1–O12 | 2.642(24) | 0.321 | O1–U1–O12 | 82.8(6) |
| $\sum S_{ij}$ | | 5.867 | | |
| | | $S_{ij}$ | | |
| U2–O8 | 1.824(13) | 1.561 | | |
| U2–O2 | 1.844(13) | 1.502 | O8–U2–O2 | 175.30(58) |
| U2–O23 | 2.154(22) | 0.811 | O8–U2–O23 | 91.22(70) |
| U2–O7 | 2.229(22) | 0.710 | O8–U2–O7 | 93.59(74) |
| U2–O6 | 2.306(22) | 0.607 | O8–U2–O6 | 92.87(75) |
| U2–O18 | 2.402(23) | 0.510 | O8–U2–O18 | 87.01(71) |
| U2–O15 | 2.599(25) | 0.347 | O8–U2–O15 | 84.88(70) |
| $\sum S_{ij}$ | | 6.048 | | |
| | | $S_{ij}$ | | |
| U3–O11 | 1.805(14) | 1.591 | | |
| U3–O3 | 1.820(14) | 1.561 | O11–U3–O3 | 177.5(6) |
| U3–O6$^{i}$ | 2.251(23) | 0.682 | O11–U3–O6$^{i}$ | 91.7(7) |
| U3–O16$^{i}$ | 2.252(23) | 0.682 | O11–U3–O16$^{i}$ | 91.5(7) |
| U3–O17 | 2.284(24) | 0.631 | O11–U3–O17 | 87.2(7) |
| U3–O7 | 2.310(21) | 0.607 | O11–U3–O7 | 91.9(7) |
| $\sum S_{ij}$ | | 5.754 | | |
| | | $S_{ij}$ | | |
| U4–O4 | 1.802(14) | 1.622 | | |
| U4–O9 | 1.841(14) | 1.502 | O4–U4–O9 | 174.5(6) |
| U4–O17$^{ii}$ | 2.240(24 | 0.695 | O4–U4–O17$^{ii}$ | 93.2(7) |
| U4–O19 | 2.288(29) | 0.631 | O4–U4–O19 | 87.8(8) |
| U4–O16 | 2.311(22) | 0.607 | O4–U4–O16 | 89.2(7) |
| U4–O21$^{iii}$ | 2.319(22) | 0.596 | O4–U4–O21$^{iii}$ | 90.7(7) |
| U4–O12$^{ii}$ | 2.385(22) | 0.520 | O4–U4–O12$^{ii}$ | 86.9(7) |
| $\sum S_{ij}$ | | 6.173 | | |
| U5–O20 | 1.746(13) | 1.786 | | |
| U5–O10 | 1.801(13) | 1.622 | O20–U5–O10 | 175.8(6) |
| U5–O7$^{ii}$ | 2.269(22) | 0.657 | O20–U5–O7$^{ii}$ | 93.4(8) |
| U5–O6 | 2.288(23) | 0.631 | O20–U5–O6 | 86.8(8) |
| U5–O18 | 2.332(22) | 0.584 | O20–U5–O18 | 91.0(8) |
| U5–O15$^{ii}$ | 2.381(22) | 0.531 | O20–U5–O15$^{ii}$ | 94.7(8) |
| $\sum S_{ij}$ | | 6.302 | | |
| *V environment* | | | | |
| | | $S_{ij}$ | | |
| V1–O22 | 1.598(22) | 1.731 | O22–V1–O14 | 112.5(8) |
| V1–O14 | 1.699(14) | 1.321 | O22–V1–O12 | 112.0(9) |
| V1–O12 | 1.735(24) | 1.218 | O14–V1–O12 | 109.3(8) |
| V1–O19 | 1.836(26) | 0.905 | O22–V1–O19 | 112.8(9) |
| $\sum S_{ij}$ | | 5.175 | O14–V1–O19 | 110.9(7) |
| V2–O13 | 1.653(14) | 1.512 | O13–V2–O21 | 108.7(8) |
| V2–O21 | 1.682(22) | 1.394 | O13–V2–O15 | 112.6(8) |
| V2–O15 | 1.718(23) | 1.251 | O21–V2–O15 | 112.9(9) |
| V2–O18 | 1.814(22) | 0.955 | O13–V2–O18 | 112.1(8) |
| $\sum S_{ij}$ | | 5.112 | O21–V2–O18 | 114.5 (9) |

Table 9 (*continued*)

| | | | | |
|---|---|---|---|---|
| *Rb environment* | | | | |
| | | $S_{ij}$ | | |
| Rb1–O3 | 2.771(19) | 0.299 | Rb2–O8$^{i}$ | 2.789(19) 0.241 |
| Rb1–O2 | 2.798(21) | 0.254 | Rb2–O11 | 2.824(21) 0.222 |
| Rb1–O5$^{ix}$ | 2.797(19) | 0.241 | Rb2–O14$^{v}$ | 2.832(23) 0.216 |
| Rb1–O3$^{ix}$ | 2.836(22) | 0.234 | Rb2–O4$^{v}$ | 2.861(19) 0.199 |
| Rb1–O10$^{i}$ | 2.907(24) | 0.210 | Rb2–O1$^{v}$ | 2.889(18) 0.184 |
| Rb1–O7 | 3.037(13) | 0.179 | Rb2–O1$^{i}$ | 2.893(23) 0.184 |
| Rb1–O17$^{ix}$ | 3.517(14) | 0.122 | Rb2–O23$^{i}$ | 3.547(17) 0.032 |
| $\sum S_{ij}$ | | 1.539 | $\sum S_{ij}$ | 1.278 |
| | | $S_{ij}$ | | |
| Rb3–O4$^{x}$ | 2.785(24) | 0.241 | Rb4–O3$^{xii}$ | 2.845(20) 0.210 |
| Rb3–O4 | 2.785(24) | 0.241 | Rb4–O3 | 2.845(20) 0.210 |
| Rb3–O1$^{ii}$ | 2.795(20) | 0.241 | Rb4–O5$^{ix}$ | 2.987(20) 0.140 |
| Rb3–O1$^{xi}$ | 2.795(20) | 0.241 | Rb4vO5$^{i}$ | 2.987(20) 0.140 |
| Rb3–O11$^{xi}$ | 2.810(18) | 0.228 | Rb4–O2$^{ix}$ | 2.991(24) 0.140 |
| Rb3–O11$^{ii}$ | 2.810(18) | 0.228 | Rb4–O2$^{i}$ | 2.991(24) 0.140 |
| Rb3–O17$^{ii}$ | 3.357(14) | 0.052 | Rb4–O23$^{ix}$ | 3.577(16) 0.028 |
| $\sum S_{ij}$ | | 1.472 | $\sum S_{ij}$ | 1.008 |
| | | $S_{ij}$ | | |
| Rb5–O20$^{x}$ | 2.770(18) | 0.254 | Rb6–O13$^{vii}$ | 2.785(23) 0.241 |
| Rb5–O4 | 2.839(21) | 0.210 | Rb6–O5 | 2.828(24) 0.216 |
| Rb5–O13$^{iii}$ | 2.845(24) | 0.210 | Rb6–O9 | 2.864(23) 0.199 |
| Rb5–O8$^{xi}$ | 2.876(19) | 0.194 | Rb6–O10$^{vii}$ | 2.927(18) 0.165 |
| Rb5–O14$^{ii}$ | 2.907(21) | 0.174 | Rb6–O2$^{vii}$ | 3.074(19) 0.110 |
| Rb5–O11$^{xi}$ | 2.973(23) | 0.148 | Rb6–O19 | 3.081(15) 0.110 |
| Rb5–O12$^{ii}$ | 3.347(15) | 0.053 | Rb6–O22 | 3.443(17) 0.042 |
| $\sum S_{ij}$ | | 1.292 | $\sum S_{ij}$ | 1.083 |
| | | $S_{ij}$ | | |
| Rb7–O13$^{xiv}$ | 2.848(19) | 0.205 | | |
| Rb7–O20 | 2.890(24) | 0.184 | | |
| Rb7–O14$^{xi}$ | 3.088(20) | 0.107 | | |
| Rb7–O8 | 3.143(23) | 0.093 | | |
| Rb7–O18 | 3.233(15) | 0.073 | | |
| Rb7–O9$^{vi}$ | 3.352(25) | 0.053 | | |
| Rb7–O10$^{xv}$ | 3.354(20) | 0.053 | | |
| Rb7–O22$^{iv}$ | 3.367(18) | 0.050 | | |
| Rb7–O21 | 3.526(17) | 0.033 | | |
| $\sum S_{ij}$ | | 0.851 | | |

Symmetry codes: (i) $-1+x,y,z$; (ii) $1+x,y,z$; (iii) $0.5+x,0.5-y,0.5+z$; (iv) $0.5+x,0.5-y,-0.5+z$; (v) $1-x,-y,-z$; (vi) $-0.5+x,0.5-y,-0.5+z$; (vii) $2-x,1-y,-z$; (viii) $1.5-x,0.5+y,-0.5-z$; (ix) $1-x,1-y,-z$; (x) $3-x,-y,-z$; (xi) $2-x,-y,-z$; (xii) $-x,1-y,-z$; (xiii) $-0.5+x,0.5-y,0.5+z$; (xiv) $1.5-x,-0.5+y,-0.5-z$; (xv) $2.5-x,-0.5+y,-0.5-z$; (xvi) $2.5-x,0.5+y,-0.5-z$.

leads to bidimensional sheets. The same bidimensional arrangement of zig-zag chains is obtained in $M_7U_8V_2O_{32}Cl$ $M$ = Rb, Cs [15], some of the shared vertices between uranium pentagonal bipyramids being replaced by chlorine atoms leading to two kinds of distorted hexagonal sites $O_6$ and $O_5Cl$, respectively. The quadrangular sites of the $O_5Cl$ rings are occupied by U atoms in distorted octahedral environment, astonishingly, for the $O_6$ rings the rectangular sites are empty while one-half of the triangular sites are occupied by V atoms.

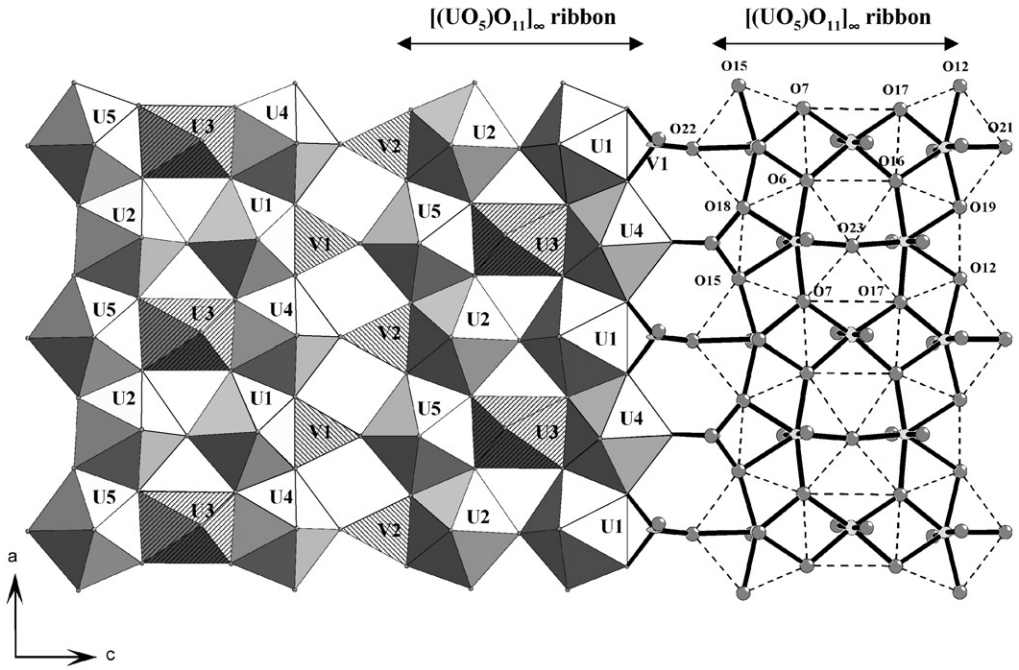


Fig. 3. Projection of the $(U_5V_2O_{23})^{6-}$ layer of $\beta$-$Rb_6U_5V_2O_{23}$ on (010) plane showing the connection of edge-shared $UO_7$ pentagonal bipyramids by $U(3)O_6$ distorted octahedra and by O(23) atoms forming $[(UO_2)_5O_{11}]_\infty$ ribbons connected together by $VO_4$ tetrahedra.

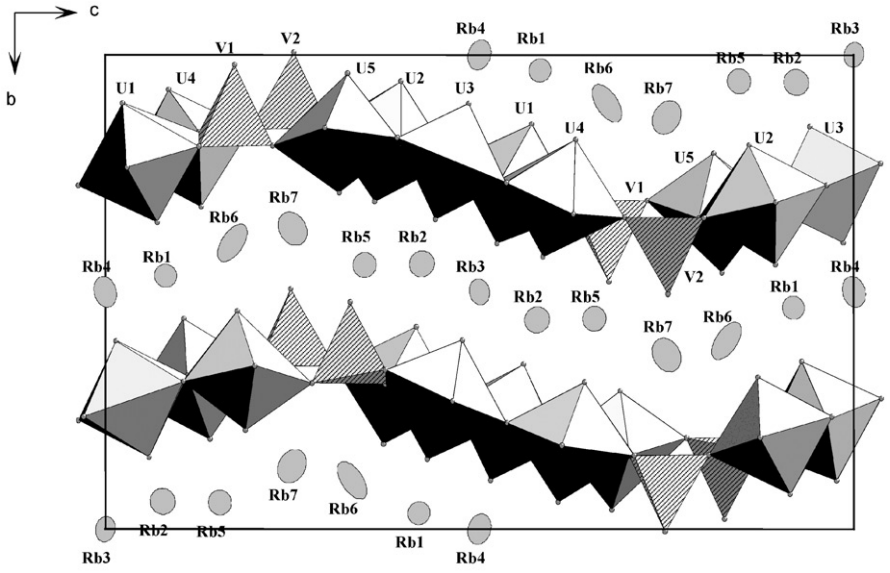


Fig. 4. The crystal structure of $\beta$-$Rb_6U_5V_2O_{23}$ projected along [100] showing parallel corrugated layers.

Another important difference between $M_6U_5V_2O_{23}$ ($M$ = Na, K, $\beta$-Rb) and $\alpha$-$Rb_6U_5V_2O_{23}$ concerns the type of connection of ribbons by $VO_4$ tetrahedra. In the first compounds, the V–O bond with the non-shared oxygen of tetrahedra connecting two consecutive ribbons are all directed towards the same interspace leading to an angle of about 40° between two consecutive ribbons. The rows of tetrahedra parallel to the [100] direction, "tip up" and "tip down", alternate leading to corrugated layers, the wave being parallel to the [001] direction. In contrast, in $\alpha$-$Rb_6U_5V_2O_{23}$, the tetrahedra "tip up" and "tip down" alternate along a row parallel to the [010] direction, leading to planar layers. This reason seems valid not only for $(U_5V_2O_{23})$ layers but also for $[UO_2(XO_4)]$ layers found in $(UO_2)_3(XO_4)_2 \cdot xH_2O$ with $X$ = P, V [33,16]. The layers are plane and apical oxygen atoms of $XO_4$ tetrahedra are alternatively pointing in both sides of the layer in each row linking two parallel $(UO_5)_\infty$ chains.

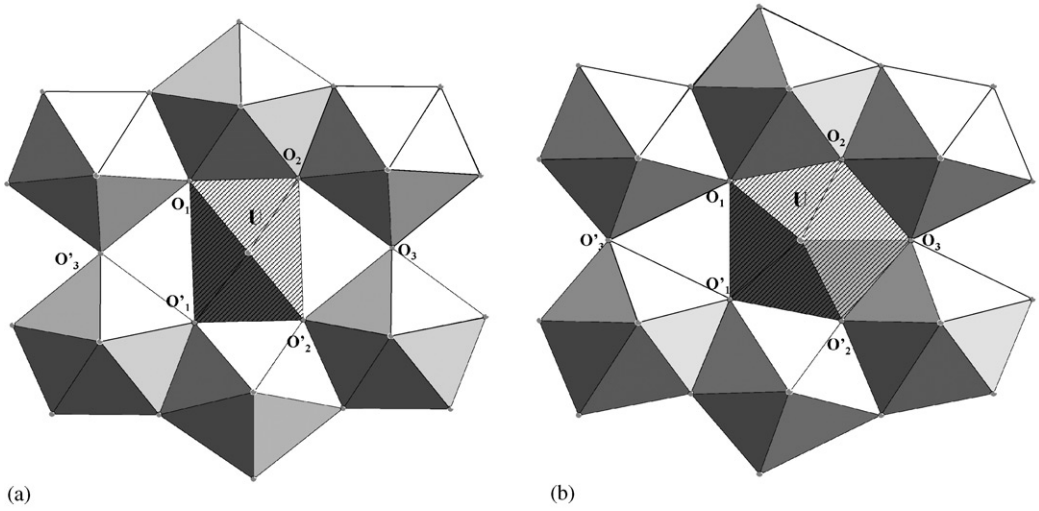


Fig. 5. Distortion of the $O_6$ rings formed between two oxygen-shared $(UO_5)_\infty$ chains from $K_6U_5V_2O_{23}$ to α-$U_3O_8$.

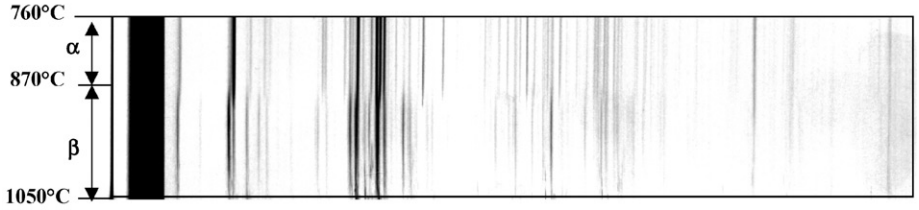


Fig. 6. High-temperature X-ray diffraction pattern of α-$Rb_6U_5V_2O_{23}$ showing a transition to the β form at about 870°C.

Table 10
Some characteristic distances and angles for the U atom occupying the $O_6$ ring between two connected $(UO_5)$ chains

| Compound | $dO_3$–$O'_3$ (Å) | Angle (deg)$O_1O_2$–$O'_1O'_2$ | $dU$–$O_3$ (Å) | $dU$–$O'_3$ (Å) |
|---|---|---|---|---|
| $K_6U_5V_2O_{23}$ | 7.135(22) | 0.000 | 3.568(18) | 3.568(18) |
| $Na_6U_5V_2O_{23}$ | 7.050(22) | 6.30(1) | 3.096(20) | 4.007(21) |
| α-$Rb_6U_5V_2O_{23}$ | 7.163(24) | 8.12(1) | 3.309(22) | 3.855(23) |
| α-$Rb_6U_5V_2O_{23}$ | 7.099(23) | 13.48(1) | 2.800(21) | 4.299(22) |
| α-$U_3O_8$ | 6.710(23) | 24.98(1) | 2.442(21) | 4.268(21) |

### 3.4. Phase transition

Thermal differential analysis performed on both α and β forms did not allow to evidence a transition between them. On the opposite, a non-reversible α to β transition is evidenced on a high-temperature X-ray diffraction pattern obtained with a Guinier–Lenné focusing camera at about 870°C, Fig. 6. This transition involves the rotation of half of the tetrahedra and is accompanied by a slight increase of the unit-cell volume.

## 4. Conclusion

The compound $Rb_6U_5V_2O_{23}$ exhibits a phase transition between α and β forms at about 870°C. Crystal growth below and above this transition allowed us to prepare single crystals of the two varieties. Both structures contains sheets of uranyl pentagonal bipyramids and $VO_4$ tetrahedra, with composition $(U_5V_2O_{23})^{6-}$. Rb ions occupy the interlayers. The main difference between the two structures concerns the $VO_4$ orientation which leads to flat and corrugated layers in the α and β forms, respectively. As a consequence the $(U_2O_9)_\infty$ ribbons formed from two $(UO_5)_\infty$ chains are more distorted in the α form leading for the U atoms occupying the holes of the ribbons to a pentagonal bipyramid coordination in the α form rather than distorted octahedron in the β form. The β form is very similar to the other $M_6U_5V_2O_{23}$ compounds with $M$ = Na, K.

## References


[1] P.B. Barton, Am. Mineral. 43 (1958) 799.
[2] M. Saadi, Ph.D. Dissertation, Université des Sciences et Technologies de Lille, France, Novembre 1994.
[3] D.E. Appleman, H.T. Evans, J. Am. Mineral. 50 (1965) 825.
[4] P.G. Dickens, C.P. Stuttard, R.G.J. Ball, A.V. Powell, S. Hull, S. Patat, J. Mater. Chem. 2 (1992) 161.
[5] F. Abraham, C. Dion, M. Saadi, J. Mater. Chem. 3 (5) (1993) 459.
[6] I.G. Zhil'tsova, S.A. Perlina, E.M. Shmariouich, Litol. Polezn. Iskop. 5 (1989) 54.
[7] F. Cesbron, Bull. Soc. Fr. Mineral. Cristallogr. 93 (1970) 320.
[8] F. Cesbron, Thèse Paris, 1970.
[9] J. Borene, F. Cesbron, Bull. Soc. Fr. Mineral. Cristallogr. 93 (1970) 426.
[10] I. Duribreux, C. Dion, F. Abraham, M. Saadi, J. Solid State Chem. 146 (1999) 258.
[11] A.M. Chippindale, S.J. Crennell, P.G. Dickens, J. Mater. Chem. 3 (1993) 33.
[12] K.J. Hilke, U.G. Brauckmann, G. Lagaly, A. Weiss, Z. Naturforsch. B 28 (1973) 239.
[13] K. Beneke, U. Grosse-Brauckmann, G. Lagaly, A. Weiss, Z. Naturforsch. B 28 (1973) 408.
[14] C. Dion, S. Obbade, E. Raekelboom, F. Abraham, M. Saadi, J. Solid State Chem. 155 (2000) 342.
[15] I. Duribreux, M. Saadi, S. Obbade, C. Dion, F. Abraham, J. Solid State Chem., in press.
[16] M. Saadi, C. Dion, F. Abraham, J. Solid State Chem. 150 (2000) 72.
[17] G. Smith, R.J. Snyder, J. Appl. Crystallogr. 12 (1979) 60.
[18] SAINT, Version 5.01. Program for Reduction of Data Collected on Bruker AXS CCD Area Detector System, Bruker Analytical X-ray Systems, Madison, WI, 1998.
[19] SABABS, Program for absorption correction using SMART CCD based on the method of Blessing, Blessing, R. H., Acta Crystallogr. A 51 (1995) 33.
[20] G.M. Sheldrick, SHELXTL PC, Version 5.0, An integrated system for Solving, Refining and Displaying Crystal Structures from Diffraction Data; Siemens Analytical X-ray Instruments, Inc., Madison, WI, 1994.
[21] M.E. Brese, M. O'Keeffe, Acta Crystallogr. B 47 (1991) 192.
[22] P.C. Burns, R.C. Ewing, F.C. Hawthorne, Can. Mineral. 35 (1997) 1551.
[23] B.O. Loopstra, Acta Crystallogr. 17 (1964) 651.
[24] L.M. Kovba, Radiokhimiya (Engl. Transl.) 13 (1971) 940.
[25] M. Gasperin, R. Chevalier, Bull. Soc. Fr. Mineral. Cristallogr. 93 (1970) 18.
[26] P.G. Dickens, G.P. Stuttard, J. Mater. Chem. 2 (1992) 691.
[27] T.L. Cremers, P.G. Eller, R.A. Penneman, C.C. Herrick, Acta Crystallogr. 39 (1983) 1163.
[28] S.V. Krivovichev, P.C. Burns, Can. Mineral. 38 (2000) 717.
[29] J.M. Jackson, P.C. Burns, Can. Mineral. 39 (2001) 187.
[30] P. Benard, D. Loüer, N. Dacheux, V. Brandel, M. Genet, Chem. Mater. 6 (1994) 1049.
[31] N. Tancret, S. Obbade, F. Abraham, Eur. J. Solid. State Inorg. Chem. 32 (1995) 195.
[32] A.M. Chipindale, P.J. Dickens, G.J. Flynnand, G.P. Stuttard, J. Mater. Chem. 5 (1) (1995) 141.
[33] A. Locock, P.C. Burns, J. Solid State Chem. 163 (2002) 275.